Feasibility of applying a tunable TEA-CO$_2$-laser-based helicopter-borne lidar to detection of methane leakages

A.I. Karapuzikov,[2] I.V. Ptashnik,[1] O.A. Romanovskii,[1] O.V. Kharchenko,[1] and I.V. Sherstov[2]

[1]*Institute of Atmospheric Optics,*
Siberian Branch of the Russian Academy of Sciences, Tomsk
[2]*Institute of Laser Physics, Siberian Branch of the Russian Academy of Sciences, Novosibirsk*

Received December 28, 1998

The spectral region near 3 μm is shown to be most promising for remote sensing of methane emissions. Parameters of radiation of a tunable repetitively-pulsed mini-TEA CO$_2$ laser and generators of its harmonics to be used in the helicopter-borne differential absorption lidar are estimated. A possibility of detecting remotely methane emissions from a pipe line is studied by numerical simulation. Possibility of detecting emissions of different intensity at a distance up to 1 km is analyzed when using third harmonic of the TEA CO$_2$ laser in an airborne lidar. The use of third harmonic of the TEA CO$_2$ laser allows methane emissions from a pipe line to be detected and measured with the mean measurement error of 10 to 15% for methane concentrations varying from its background level to the explosion-hazardous one.

Introduction

In connection with rapid development of oil and gas industry, the problem of detecting gaseous emissions from pipe lines becomes increasingly urgent, especially in view of high ecological danger of such emissions. Therefore, it becomes of primary importance to develop the corresponding methods for analysis of the local gaseous composition of the atmosphere. These methods should ensure fast data acquisition on the atmospheric composition on large scales.

Laser methods of sensing gaseous constituents of the atmosphere most completely satisfy the above requirements. Since resonance absorption has the largest interaction cross section, the laser differential absorption (DIAL) method, which employs this effect, exhibits high sensitivity.

Background

Sensing of methane with DIAL method allows the use of methane absorption bands from the near and mid-infrared spectral regions. Table 1 presents spectroscopic parameters for such bands. The parameters presented have been borrowed from Ref. 1.

Table 1. Spectroscopic parameters of the methane (C^{12}H$_4$) absorption bands.

No.	Total number of lines	ν_{min}, cm^{-1}	ν_{max}, cm^{-1}	I_{min}, cm/molecule	I_{max}, cm/molecule	I_{sum}, cm/molecule
1	4017	944.397	1627.974	$2.30 \cdot 10^{-27}$	$9.68 \cdot 10^{-20}$	$5.14 \cdot 10^{-19}$
2	2397	1109.032	1605.075	$4.04 \cdot 10^{-26}$	$3.82 \cdot 10^{-22}$	$3.65 \cdot 10^{-20}$
3	2641	1163.297	1865.705	$5.94 \cdot 10^{-28}$	$1.03 \cdot 10^{-21}$	$5.44 \cdot 10^{-20}$
4	1266	2255.492	2847.219	$1.32 \cdot 10^{-24}$	$8.39 \cdot 10^{-22}$	$5.50 \cdot 10^{-20}$
5	839	2511.381	3175.006	$1.00 \cdot 10^{-24}$	$1.10 \cdot 10^{-21}$	$1.45 \cdot 10^{-20}$
6	2300	2573.104	3167.121	$1.22 \cdot 10^{-24}$	$5.18 \cdot 10^{-21}$	$3.78 \cdot 10^{-19}$
7	1903	2809.527	3209.941	$1.48 \cdot 10^{-24}$	$2.13 \cdot 10^{-19}$	$1.08 \cdot 10^{-17}$
8	712	2880.787	3153.543	$2.20 \cdot 10^{-24}$	$6.17 \cdot 10^{-22}$	$4.45 \cdot 10^{-20}$
9	754	2919.131	3253.323	$1.00 \cdot 10^{-24}$	$7.16 \cdot 10^{-22}$	$3.40 \cdot 10^{-20}$
10	172	4136.164	4278.242	$1.90 \cdot 10^{-22}$	$5.24 \cdot 10^{-21}$	$2.40 \cdot 10^{-19}$
11	958	4147.844	4489.169	$1.56 \cdot 10^{-23}$	$5.53 \cdot 10^{-21}$	$4.08 \cdot 10^{-19}$
12	388	4409.945	4666.559	$2.05 \cdot 10^{-23}$	$1.21 \cdot 10^{-21}$	$6.24 \cdot 10^{-20}$
13	144	5991.066	6106.295	$4.06 \cdot 10^{-23}$	$1.32 \cdot 10^{-21}$	$5.97 \cdot 10^{-20}$

As seen from Table 1 and Fig. 1, the strongest band is that centered near 3 μm (~ 3000 cm^{-1}, band No. 7 with the total intensity of $1.08 \cdot 10^{-17}$ cm·molecule^{-1}). This band opens up wide possibilities for selecting optimal wavelengths for sensing the background and enhanced concentrations of methane. Besides, several absorption bands with lower intensity also fall within this range (bands Nos. 4 − 6, 8, and 9). This allows us to find informative wavelengths for sensing methane emissions with high concentration, which exceeds the background one by several orders of magnitude.
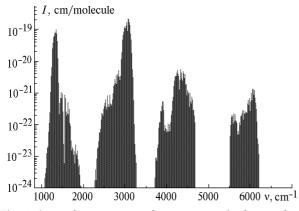
Fig. 1. Spectral position and intensity of the methane absorption bands.

There are also methane absorption bands centered near 7.5 μm (~ 1300 cm^{-1}, bands Nos. 1 − 3), 2.2 μm (~ 4500 cm^{-1}, bands Nos. 10 − 12), and 1.66 μm (~ 6000 cm^{-1}, band No. 13). However, their intensity is two to three orders of magnitude lower. This fact allows these bands to be used for lidar sensing of methane only at very high methane concentrations (higher than 50−100 ppm).

Methane measurements by DIAL method are currently implemented for the open-path scheme with a mirror reflector using the He−Ne laser wavelengths of 3.3922 μm (2947.9394 cm^{-1}) and 3.3912 μm (2948.8087 cm^{-1}), which are used as basic and reference wavelengths, respectively.[2] However, application of this laser, having relatively low output power (tens milliwatts), in lidar measurements with a topo-target as a reflector is feasible only for paths no longer than 100 to 150 m. Sensing from such a short distance may be dangerous in the case of extremely intense methane emissions.

Reference 3 reports on measurements of methane concentration by DIAL method with the use of Nd:YAG-laser radiation converted into the 3-μm spectral region with an optical parametric oscillator. In this case, radiation at 3.313 μm (3018.41 cm^{-1}) was used as a basic wavelength, and radiation at 3.309 μm (3022.06 cm^{-1}) served a reference wavelength. Upon calculation of the absorption spectra, we have shown that the wavelengths proposed in Ref. 3 can be used for sensing only with regard for correction for the strong interfering effect from absorption by water vapor and at low methane concentrations (no higher than 10 to 20 ppm).

On the other hand, Ref. 4 reports on successful implementation of an airborne (helicopter-borne) open-path analyzer of ammonia with the use of fundamental harmonic of a cw tunable CO$_2$ laser. This allowed successful mapping and identification of sources of ammonia emissions along a gas pipe line and in the vicinity of a chemical plant.

In Ref. 5, the authors have proposed the third-harmonic CO$_2$-laser radiation to be used for detection of methane leakage. However, this reference gives no particular estimates of the capabilities of such a radiation source for lidar sensing by DIAL method.

The aim of this work is to estimate numerically (based on numerical simulation) possibilities of remotely detecting methane emissions from pipe lines. We have analyzed the possibility of detecting methane emissions at a distance up to 1 km with the use of third harmonic of the TEA CO$_2$ laser in a lidar installed on board a helicopter.

Selection of the radiation source for the helicopter-borne open-path gas analyzer

Let us estimate some necessary power and spectral parameters of radiation for the helicopter-borne open-path gas analyzer intended for detection of methane leakage from gas pipe lines. Methane is an explosive gas, therefore its sensing from onboard a helicopter should be conducted at a safe distance as long as 1 km. Figure 2 shows the sensing scheme. In this scheme, the helicopter flies at a velocity of 40 m/s (about 150 km/h) at the altitude h = 700 m along the pipe line at a distance R = 700 m from it. An optical beam propagates from the helicopter down to the surface at an angle α = 135° to zenith. The length of the sensing path L in this case is 1 km.
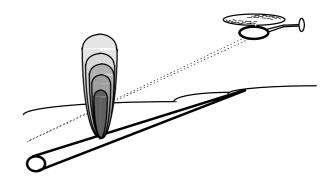

Fig. 2. Scheme of lidar sensing of methane from onboard a helicopter.

Lidar returns acquired in a sensing session are accumulated and averaged for several pairs of laser pulses in order to increase the signal-to-noise ratio. Assume that return signals can be accumulated only for some time interval τ, during which the helicopter covers the distance ΔR, comparable with the size of a laser foot print on the Earth's surface. In that case, we can state that practically the same section of the path sounded is within the field of view of the lidar receiver. Let us take the divergence of a sounding beam $2\theta_t$ = 3 mrad and the entire field-of-view angle of the lidar receiver $2\theta_r$ = 4 mrad. Thus, the diameter of the laser foot print on the Earth's surface at the distance L = 1 km is equal to 3 m. So it takes a helicopter flying at a speed v = 40 m/s only Δt = 0.075 s to cover the distance ΔR = 3 m. Therefore we can take the time of signal accumulation τ = 0.1 s. Assume that for the time τ, the total of n = 10 pairs of pulses, i.e.

20 pulses, must be accumulated. Thus, the minimum pulse repetition rate f and the rate of tuning laser radiation acceptable for a helicopter-borne open-path gas analyzer is 200 Hz. It should also be noted that the delay between two consecutive pulses at this pulse repetition rate is $\Delta t = 5$ ms, what meets the condition of "frozenв atmospheric turbulence.

Radiation of a tunable laser in the spectral region from 3.1 to 3.6 μm can be obtained by efficient frequency conversion of a repetitively pulsed TEA CO_2 laser to the third harmonic of its fundamental line. Nowadays noticeable results have been achieved in generation of harmonics and combination frequencies of CO_2-laser radiation. Thus, for example, Chou et al.[6] succeeded in generation of the fourth harmonic of CO_2 laser at 2.38 μm using a tandem of $AgGaSe_2-ZnGeP_2$ nonlinear crystals. The efficiency of this conversion was about 10%. Harasaki et al.[7] reported on generation of the third harmonic of repetitively pulsed TEA CO_2-laser ($10p(20)$ line) in $AgGaSe_2$ crystals with the total efficiency of 10%. Besides, in Ref. 7 about 40% of power of the second harmonic was converted to the third harmonic radiation.

Let us consider the feasibility of using a repetitively pulsed mini-TEA CO_2 laser as a radiation source for the helicopter-borne open-path gas analyzer of methane. In this paper we consider a laser with the pulse energy $E_0 = 20$ mJ, pulse duration at FWHM $\tau_{FWHM} = 50$ ns, and pulse repetition rate $f = 200$ Hz. As a generator of the third harmonic, we consider that based on $AgGaSe_2$ or $ZnGeP_2$ crystal with the conversion efficiency $\eta = 5\%$. In this case, the third-harmonic radiation pulse of the mini-TEA CO_2 laser has the energy $E_3 = 1$ mJ at the wavelength of 3 μm. This energy corresponds to the pulse power $P_t = 20$ kW at 50-ns FWHM pulse duration.

Let us estimate the power of the lidar return signal P_s recorded by the lidar receiver. In a simplified form, the expression for P_s can be written as

$$P_s = P_t \, K_t \, K_r \, r_a \, T_a \, (S / 2\pi L^2) , \qquad (1)$$

where P_t is the power of a sounding pulse; K_t is the efficiency of the transmitting optics; K_r is the efficiency of the receiving optics (including the spectral filter); r_a is the coefficient of diffuse reflection from the Earth's surface (albedo); T_a is the atmospheric transmittance; $S = \pi a^2$ is the area of an objective lens of the receiving telescope, $2\pi L^2$ is the area of the upper hemisphere of space at the distance L. To estimate P_s, let us take the following typical values: $K_t = 0.7$, $K_r = 0.4$, $r_a = 0.05$, $T_a = e^{-1} = 0.37$, $S = 0.03$ m^2 at the receiving telescope aperture $2a = 0.2$ m, $L = 1000$ m. With the above-listed parameters in mind and with a lidar transmitter emitting $P_t = 20$ kW power, the estimated value of the recorded lidar return signal is as $P_s = 520$ nW.

Consider the value of the noise component N_b due to background radiation. It is described by the expression

$$N_b = B \, S \, (\pi \theta_r^2) \, \Delta\lambda \, K_r , \qquad (2)$$

where B is the background radiation; $\pi\theta_r^2$ is the solid angle of the receiver's field of view; $\Delta\lambda$ is the bandwidth of a spectral filter. Having substituted the values $\theta_r = 2$ mrad, $b = 0.003$ W/(m^2·sr·nm), and $\Delta\lambda = 30$ nm in Eq. (2), we obtain the power of the background radiation $N_b = 14$ nW.

Small-size InAs detectors are preferable to be used because they do not require cooling with liquid nitrogen. Thus, for example, J12TE2−8B6−R01M InAs detector (manufactured by EG&G Judson, Canada) has a sensitive area of 1 mm in diameter and two stages of cooling (the working temperature of the crystal $T = -40°C$), as well as possesses NEP = 2.9 pW/Hz$^{1/2}$ and the time constant $\tau < 50$ ns. At the bandwidth of the electronics $\Delta f = 10$ MHz, the power of noise due to NEP of this detector is $N_d = 9$ nW.

The resulting total noise power in a single measurement of the return signal is $N = N_d + N_b = 23$ nW, and the signal-to-noise ratio is 520 nW/23 nW ≈ 23. As return signals are accumulated for 10 pairs of pulses, the signal-to-noise ratio increases by a factor of $\sqrt{10}$ and becomes ≈ 71, that is, noise contributes about 1.4%.

Thus, summarizing the above-said, we can conclude that to be used in the helicopter-borne lidar for remote detection of methane leakage from pipe lines at the distance of 1 km, the laser should met the following requirements. It should be a small-size tunable repetitively pulsed TEA CO_2 laser with the pulse repetition rate and the rate of tuning no less than 200 Hz, and the pulse energy no less than 20 mJ at 50-ns pulse duration (FWHM). The third-harmonic generator with the conversion efficiency no less than 5% is also required. The mini-TEA CO_2 laser described in Ref. 8 meets all the above requirements.

In the Institute of Laser Physics SB RAS (Novosibirsk), fast-tunable repetitively pulsed mini-TEA CO_2 laser is being developed for operation with the third-harmonic generator as a part of an airborne differential absorption lidar for remote detection of methane leakage from pipe lines. The laser emits short pulses in the spectral region from 9.2 to 10.8 μm with the pulse repetition rate and the tuning rate as high as 400 Hz. The energy of laser pulses at strong lines achieves 50 mJ, and the peak output power is about 500 kW.

Development of the mini-TEA CO_2 laser is based on the experimental results obtained at the Institute of Laser Physics SB RAS when studying and optimizing output parameters of high-power TEA CO_2 laser with the pulse energy of 1 to 9 J. This laser has been designed for use in a ground-based differential absorption lidar for atmospheric monitoring within the range from 10 to 15 km (Ref. 10).

A unique part of the mini-TEA CO_2 laser under development is the optimized gas-dynamic system for fast cross circulation of a gas mixture through the

discharge gap. This system allows the mini-TEA CO_2 laser to operate at a high pulse repetition rate. A highly efficient diametrical fan provides for fast circulation of the gas mixture. The laser employs a CO_2:N_2:He:H_2 gas mixture at different ratios of gases and at the total pressure close to the atmospheric pressure or higher.

The laser cavity configuration is similar to the resonator described in Ref. 9. The selective resonator of the mini-TEA CO_2 laser is L-shaped. It comprises an immovable diffraction grating, an exit mirror, and rotatable polyhedral mirror. The rotatable mirror directs the optical beam onto the diffraction grating at different incidence angles to tune the wavelength in the range from 9.2 to 10.8 μm with the tuning rate up to 400 Hz. At high rate of mirror rotation, a "tailВ of the laser pulse is cut off because of mechanical misalignment of the resonator, what results in a shorter duration of laser pulses.

The airborne lidar consists of two units. The optical unit with the size of 500×600×700 mm includes a mini-TEA CO_2 laser, a third-harmonic generator, and the optical transmitter-receiver of the lidar. The lidar receiver comprises a Newtonian telescope with a 200-mm-diameter aperture, an InAs detector with a micro-cooler, and changeable spectral filters. The lidar's electronic unit includes the pulsed power supply for the laser, electronic control units, and a cooler. The lidar is operated from +27 V power source; power consumption is about 1 kW.

The radiation of a mini-TEA CO_2 laser is converted into the third harmonic with the AgGaSe$_2$ or ZnGeP$_2$ nonlinear crystals with the efficiency of 5 to 10%. The resulting laser beam with the divergence $2\theta_t = 3$ mrad has the following spectral and power parameters:

wavelength region, nm	3040−3645
halfwidth, nm	0.1−0.2
pulse repetition rate, Hz	400
pulse duration at FWHM, ns	50
pulse energy (third harmonic), mJ	1−2
peak power (third harmonic), kW	20−40
wavelength instability, nm	0.02

Results of numerical simulation

SAGDAM software

The SAGDAM (Sounding of Atmospheric Gases by Differential Absorption Method) interactive software[11] was designed for simulation of laser sensing of atmospheric gases by the differential absorption method along vertical and slant paths with ground-based and airborne lidars. The SAGDAM software seeks optimal pairs of wavelengths for sensing and calculates error profiles for them.

Initially, the SAGDAM program package has been developed for simulations in sensing with a quasi-monochromatic radiation, i.e., a source such that the width of a spectral line of radiation from it is far narrower than the width of absorption lines of a gas

analyzed. The laser radiation nonmonochromaticity was considered only as one of the systematic errors of sensing. However, here we deal with a high-power TEA CO_2 laser with the pressure of the working mixture up to 2 atm. So the calculation scheme has been modified to correctly take into account the width of laser line both in calculating the absorption spectra and in determination of the effective (in this case) coefficients of gas absorption.[12]

Initial data

As the initial data, the SAGDAM package used the following parameters.

1) Path geometry is shown in Fig. 2 for the helicopter-borne lidar sensing of methane. The lidar altitude was taken to be 700 m, the sensing angle (from zenith) was 135°. With this geometry, the path length (from lidar to the target) was 1 km. The mean albedo of the target was taken 10% (Ref. 13).

2) Parameters of the third harmonic of the fast-tunable mini-TEA CO_2 laser have just been presented above.

3) Receiver:

receiving aperture of the telescope, m^2	0.03;
transmitting aperture, m^2	0.01;
field-of-view angle of the receiving telescope, mrad	3;
optical filter bandwidth, nm	20;
electronics bandwidth, MHz	50;
time of signal accumulation, s	0.1;
transmittance of the receiving and transmitting optics,	0.5;
error in measurement of a single lidar return, %	10;
NEP of the photodetector (based on InSb|$_{LN2}$ (Ref. 14)), W/Hz$^{1/2}$	$1 \cdot 10^{-12}$.

4) Meteorological model: the standard mid-latitude summer model (IAO model).[15] The background content of methane and water vapor (as of an analyzed and foreign gases) in the surface atmospheric layer was taken 1.5 ppm and $1.5 \cdot 10^4$ ppm, respectively. A simulated plume of the methane emission near a pipe line was taken to have 100 m diameter. In the process of simulation, the methane content in the cloud varied from the background level (1.5 ppm) to the nearly explosion-hazardous one (15000 ppm).

5) For the aerosol model we took the optical model of the continental aerosol.[16]

6) Background radiation: for the upper estimate of the signal error due to neglecting the background, the differential background irradiance was assumed equal to 0.003 W/(sr·m^2·nm). This value corresponds to 10% (albedo) for solar radiation reflected from the Earth's surface.

Optimal pairs of sounding radiation wavelengths

The numerical simulation with the SAGDAM software has allowed us to select four pairs of wavelengths for sensing of methane. The information about these wavelengths is given in Table 2. Table 2 presents four optimal pairs of wavelengths: two pairs

are in the 10R branch and another two pairs are in the 9P branch. Besides, these wavelengths are among most intense lasing lines of a CO_2 laser (lines from 12th to 20th). Table 2 presents also the values of the effective differential absorption coefficient ΔK for the selected pairs of wavelengths. The values differ by more than an order of magnitude, what is connected with the need to detect methane in a wide concentration range. When simulating methane concentration in a 100-m zone of emission, the concentration was varied from the background level of 1.5 ppm to the nearly explosion-hazardous level ~15000 ppm (see Tables 2−4).

It can also be seen from Table 2 that the optical filter bandwidth of 20−30 cm^{-1} (20−30 nm) is sufficient for use with any of two pairs of wavelengths (in 10R or 9P branch). Absorption spectra of methane and foreign gases, as well as spectral positions of the third harmonics of the selected optimal pairs are shown in Figs. 3 and 4. As seen, radiation absorption by foreign gases at the selected wavelengths is low as

compared with the effective differential absorption coefficient of methane.

Analysis of sensing errors

The SAGDAM software package has allowed us to analyze expected errors of sensing of methane emissions at the selected pairs of wavelengths. The results of analysis are given in Tables 3 and 4. The Tables present the methane concentration ρ_{CH_4} in a 100-m-thick plume (first column), the optimal pair of wavelengths for sensing (second column), the value of ΔK for this concentration of methane in the zone of emission (third column), the on-line transmittance for the selected pair of wavelengths $T_{\Delta\nu}$ (fourth column), the total error in determination of the methane content ε_{Σ} (fifth column), the error in signal (sixth column), the error due to the effect of foreign gases (seventh column), and the error due to uncertainty in calculation of the absorption coefficient $\varepsilon_{\delta K}$ (eighth column).

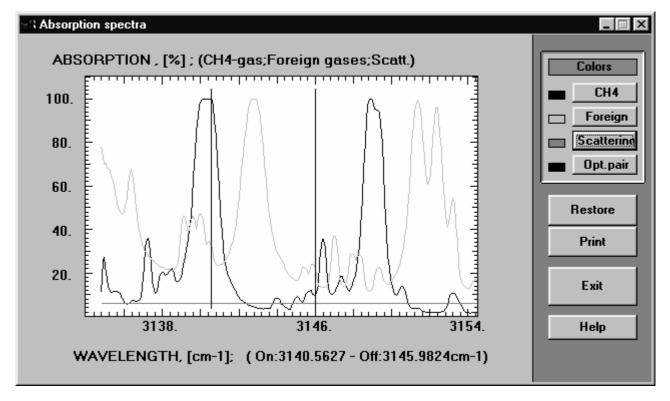**Table 2. Optimal pairs of wavelengths for sensing of methane.**

Number	ρ_{CH_4}, ppm	ν_{on}, cm^{-1}	ν_{off}, cm^{-1}	N_{on}	N_{off}	ΔK, cm$^{-1} \cdot$ atm^{-1}
1	1.5−250	2927.7913	2923.8657	10R(20)	10R(18)	1.74−0.94
2	500−5000	2919.8655	2911.6416	10R(16)	10R(12)	0.07−0.05
3	1.5−250	3140.5627	3145.9824	9P(20)	9P(18)	1.8−1.14
4	500−15000	3156.5867	3161.7705	9P(14)	9P(12)	0.03−0.026

Table 3. Results of numerical simulation of methane emissions sensing with radiation near the third harmonic of the _P_-branch of the CO_2 laser.
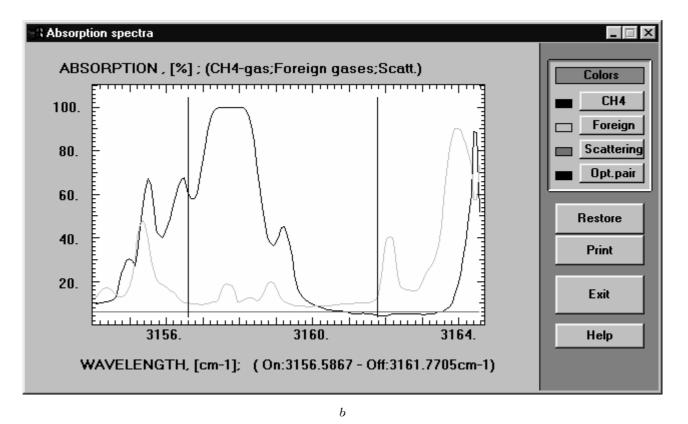
ρ_{CH_4}, ppm	Optimal pair, cm^{-1}	ΔK, cm$^{-1}\cdot$atm^{-1}	$T_{\Delta\nu}$	ε_{Σ}, %	ε_s, %	$\varepsilon_{f.g.}$ %	$\varepsilon_{\delta K}$, %
1.5	$3 \times 9P(20) - 3 \times 9P(18)$	1.8	0.60	40	6	39	10
250	3140.5627−3145.9824	1.14	0.004	14	10	4	9
500		0.030	0.75	19	11	13	8
1500	$3 \times 9P(14) - 3 \times 9P(12)$	0.029	0.40	8	3.7	4	6
5000	3156.5867−3161.7705	0.028	0.06	6	1.2	1.4	6
15000		0.026	0.0004	7	2.5	0.5	6

Table 4. Results of numerical simulation of methane emissions sensing with radiation near the third harmonic of the _R_-branch of the CO_2 laser.
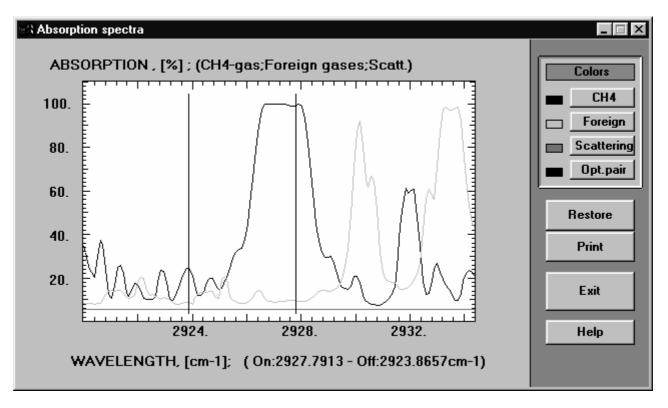
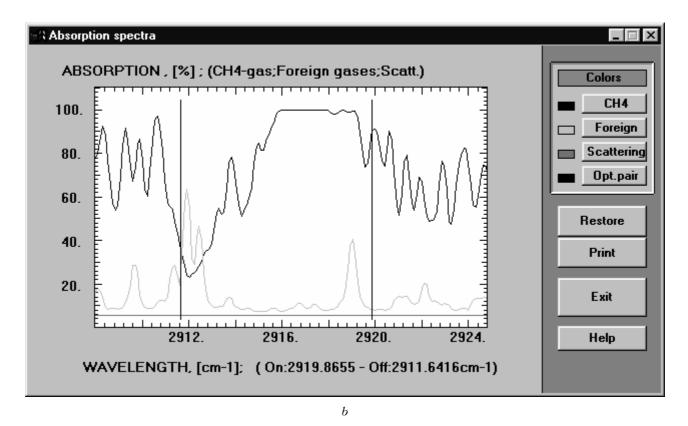| ρ_{CH_4}, ppm	Optimal pair, cm^{-1}	ΔK, cm$^{-1}\cdot$atm^{-1}	$T_{\Delta\nu}$	ε_{Σ}, %	ε_s, %	$\varepsilon_{f.g.}$ %	$\varepsilon_{\delta K}$, %
1.5	$3 \times 10R(20)-3 \times 10R(18)$	1.74	0.58	11	7	4	7.5
250	2927.7913−2923.8657	0.94	0.008	30	27	0.4	11.5
500		0.071	0.43	16	4.5	12.0	8
1500	$3 \times 10R(16)-3 \times 10R(12)$ 2919.8655−2911.6416	0.061	0.10	9.6	1.8	5	8
5000		0.046	0.002	12	5.4	2.0	10

a

b

Fig. 3. Absorption spectrum of methane (solid curve) and water vapor (dotted curve), and spectral positions of the $9P(20)$ and $9P(18)$ lines of the third harmonic of the CO_2 laser for the methane concentration of 250 ppm (*a*) and those for $9P(14)$ and $9P(12)$ lines for the methane concentration of 1500 ppm (*b*).

a

b

Fig. 4. Absorption spectrum of methane (solid curve) and water vapor (dotted curve), and spectral positions of the 10R(20) and 10R(18) lines of the third harmonic of the CO_2 laser for the methane concentration of 250 ppm (*a*) and those for 10R(16) and 10P(12) lines for the methane concentration of 1500 ppm (*b*).

As seen from the Tables, the selected optimal pairs of wavelengths corresponding to absorption lines of different intensity allow identification of methane emissions through the entire concentration range from 1.5 to 15000 ppm. The total error does not exceed 20%, if the methane concentration in the zone of emission is higher than 15–20 ppm. In the case of background methane concentration, the errors for the pair $3 \times 9P(20) - 3 \times 9P(18)$ may reach several tens percent. In this connection, one have to use either the pair $3 \times 10R(20) - 3 \times 10R(18)$ or stronger absorption lines of CH_4, for example, the line centered at 3018.16 cm^{-1}, which coincides with the third harmonic of the $9p(14)$ line of $C^{13}O_2^{16}$ laser.[5]

Conclusions

1. The 3-μm spectral region rich in CH_4 absorption lines of different intensity is much promising for remote sensing of methane emissions in the atmosphere.

2. It is worth using the third harmonic of a tunable mini-TEA CO_2 laser as a source of laser radiation. The third harmonic can be obtained by efficient frequency conversion in AgGaSe$_2$ or ZnGeP$_2$ nonlinear crystals. The use of the third harmonic allows obtaining of laser pulses with the energy of 2 to 5 mJ in the spectral region from 3040 to 3645 nm at the pulse repetition rate of 400 Hz as high.

3. The use of third harmonic of a TEA CO_2 laser opens the possibility of detecting methane emissions from pipe lines with an airborne differential absorption lidar. The error in measured methane concentrations does not exceed 10 to 15% at the methane concentrations from the background level up to near explosion-hazardous level. Only two pairs of wavelengths: $10R(20) - 10R(18)$ and $10R(16) - 10R(12)$ or $9P(20) - 9P(18)$ and $9P(14) - 9P(12)$ are sufficient for such a detection.

References

1. L.S. Rothman, R.R. Gamache, R.N. Tipping, et al., J. Quant. Spectrosc. Radiat. Transfer **48**, 469–507 (1992).
2. V.I. Astakhov, A.S. Burmistrov, V.V. Galaktionov, et al., Opt. Atm. **1**, No. 10, 65–69 (1988).
3. S.G. Anderson, Laser Focus World, No. 12, 15–16 (1995).
4. V.V. Berezovskii, A.L. Gandurin, E.A. Igumnov, et al., Kvant. Elektron. **14**, No. 9, 1917–1920 (1987).
5. P.P. Geiko, O.A. Romanovskii, O.V. Kharchenko, and S.F. Shubin, *"Capabilities of Application of Frequency-Converted Radiation of* CO *and* CO$_2$ *Lasers to Gas Analysis of the Atmosphere by the Differential Absorption Method*, BVINITI, No. 6378–b 90, December 21, 1990, Moscow (1990), 36 pp.
6. H.P. Chou, R.S. Slater, and Y. Wang, Appl. Phys. **B66**, 555–559 (1998).
7. A. Harasaki, J. Sakuma, T. Itoh, et al., Proc. SPIE **3125**, 410–418 (1997).
8. D. Cohn, J. Fox, and C. Swim, Proc. SPIE **2118**, 72–82 (1994).
9. J. Fox and J.L. Ahl, Appl. Opt. **25**, No. 21, 3830–3834 (1986).
10. Yu.M. Andreev, A.I. Karapuzikov, I.A. Razenkov, et al., in: *Abstracts of Reports at the International Symposium on Monitoring and Rehabilitation of the Environment*, Tomsk (1998), pp. 15–18.
11. K.M. Firsov, M.Yu. Kataev, A.A. Mitsel', I.V. Ptashnik, and V.V. Zuev, J. Quant. Spectrosc. Radiat. Transfer **61**, No. 1, 25–37 (1999).
12. V.V. Zuev, A.A. Mitsel', and I.V. Ptashnik, Atmos. Oceanic Opt. **5**, No. 9, 631–635 (1992).
13. I.S. Grigor'ev and E.Z. Meilikhov, eds., *Physical Constants* (Energoatomizdat, Moscow, 1991), 259 pp.
14. M.W. Sigrist, ed., *Air Monitoring by Spectroscopic Techniques. Chemical Analysis* (Wiley-Interscience Publication, 1994), Vol. 127, 335 pp.
15. V.E. Zuev and V.S. Komarov, *Statistical Models of Temperature and Gaseous Constituents of the Atmosphere* (Gidrometeoizdat, Leningrad, 1986), 264 pp.
16. G.M. Krekov and R.F. Rakhimov, *Optical Lidar Model of the Continental Aerosol* (Nauka, Novosibirsk, 1982), 199 pp.